

AD-A206 124

4  
CHEMICAL  
RESEARCH,  
DEVELOPMENT &  
ENGINEERING  
CENTER

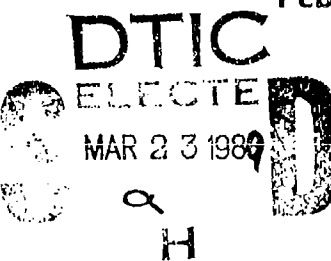
CRDEC-TR-045

THE DYNAMIC BEHAVIOR OF WATER VAPOR  
ON ACTIVATED CARBON

John J. Mahle  
RESEARCH DIRECTORATE

David K. Friday  
GEO-CENTERS, INC.  
Ft. Washington, MD 20744

February 1989



U.S. ARMY  
ARMAMENT  
MUNITIONS  
CHEMICAL COMMAND

Aberdeen Proving Ground, Maryland 21010-5423

DISTRIBUTION STATEMENT A  
Approved for public release  
Distribution Unlimited

30 2 00 750

**Disclaimer**

The findings in this report are not to be construed as an official Department of the Army position unless so designated by other authorizing documents.

**Distribution Statement**

Approved for public release; distribution is unlimited.

## UNCLASSIFIED

SECURITY CLASSIFICATION OF THIS PAGE

Form Approved  
OMB No. 0704-0188

REPORT DOCUMENTATION PAGE			
1a. REPORT SECURITY CLASSIFICATION UNCLASSIFIED		1b. RESTRICTIVE MARKINGS	
2a. SECURITY CLASSIFICATION AUTHORITY		3. DISTRIBUTION/AVAILABILITY OF REPORT Approved for public release; distribution is unlimited.	
2b. DECLASSIFICATION/DOWNGRADING SCHEDULE			
4. PERFORMING ORGANIZATION REPORT NUMBER(S) CRDEC-TR-045		5. MONITORING ORGANIZATION REPORT NUMBER(S)	
6a. NAME OF PERFORMING ORGANIZATION See Reverse		6b. OFFICE SYMBOL (if applicable)	7a. NAME OF MONITORING ORGANIZATION
6c. ADDRESS (City, State, and ZIP Code)		7b. ADDRESS (City, State, and ZIP Code)	
8a. NAME OF FUNDING / SPONSORING ORGANIZATION CRDEC		8b. OFFICE SYMBOL (if applicable) SMCCR-RSC-A	9. PROCUREMENT INSTRUMENT IDENTIFICATION NUMBER DAAA15-87-D-0007
8c. ADDRESS (City, State, and ZIP Code) Aberdeen Proving Ground, MD 21010-5423		10. SOURCE OF FUNDING NUMBERS	
		PROGRAM ELEMENT NO.	PROJECT NO.
		1C161102	A71A
		WORK UNIT ACCESSION NO.	
11. TITLE (Include Security Classification) The Dynamic Behavior of Water Vapor on Activated Carbon			
12. PERSONAL AUTHOR(S) Mahle, John J. (CRDEC); and Friday, David K. (GEO-Centers, Inc.)			
13a. TYPE OF REPORT Technical	13b. TIME COVERED FROM 87 Feb TO 88 Jul	14. DATE OF REPORT (Year, Month, Day) 1989 February	15. PAGE COUNT 30
16. SUPPLEMENTARY NOTATION			
17. COSATI CODES		18. SUBJECT TERMS (Continue on reverse if necessary and identify by block number)	
FIELD 15	GROUP 06	SUB-GROUP 03	Breakthrough Water vapor Activated carbon
			Simulation Stage model Equilibrium theory
19. ABSTRACT (Continue on reverse if necessary and identify by block number) Water vapor is present, usually in relatively large concentrations, in many adsorption systems of industrial and military interest. This work develops an approach to predict the dynamic behavior of water vapor on an activated carbon adsorbent. Prior studies have neglected the importance of including the heat balance to account for behavior to high relative humidities.			
Water vapor isotherms were measured for BPL carbon at 15, 25, and 35 °C, and the data were correlated using a modified version of the Antoine Equation first suggested by LeVan. Breakthrough experiments were performed using the following initial bed and feed conditions: (1) 50% RH feed to a dry bed, (2) 80% RH feed to a bed initially equilibrated at 50% RH, and (3) 80% RH feed to a dry bed. Two mathematical models were developed to analyze the values predicted using a non-isothermal stage model with a fluid phase mass transfer resistance and an adiabatic equilibrium theory model. (AW)			
20. DISTRIBUTION/AVAILABILITY OF ABSTRACT <input checked="" type="checkbox"/> UNCLASSIFIED/UNLIMITED <input type="checkbox"/> SAME AS RPT <input type="checkbox"/> DTIC USERS		21. ABSTRACT SECURITY CLASSIFICATION UNCLASSIFIED	
22a. NAME OF RESPONSIBLE INDIVIDUAL SANDRA J. JOHNSON		22b. TELEPHONE (Include Area Code) (301) 671-2914	22c. OFFICE SYMBOL SMCCR-SPS-T

UNCLASSIFIED

6. NAME AND ADDRESS OF PERFORMING ORGANIZATION (Continued)

U.S. Army Chemical Research, Development and Engineering Center  
ATTN: SMCCR-RSC-A  
Aberdeen Proving Ground, MD 21010-5423

GEO-Centers, Inc.  
10903 Indian Head Highway  
Ft. Washington, MD 20744

## PREFACE

The work described in this report was authorized under Project No. 1C161102A71A, Research in CW/CB Defense, and Contract No. DAAA15-87-D-0007. This work was started in February 1987 and completed in July 1988.

The use of trade names or manufacturers' names in this report does not constitute an official endorsement of any commercial products. This report may not be cited for purposes of advertisement.

Reproduction of this document in whole or in part is prohibited except with permission of the Commander, U.S. Army Chemical Research, Development and Engineering Center, ATTN: SMCCR-SPS-T, Aberdeen Proving Ground, Maryland 21010-5423. However, the Defense Technical Information Center and the National Technical Information Service are authorized to reproduce the document for U.S. Government purposes.

This report has been approved for release to the public.



Accession For	
NTIS GRA&I	<input checked="" type="checkbox"/>
DTIC TAB	<input type="checkbox"/>
Unannounced	<input type="checkbox"/>
Justification	
By	
Distribution	
Availability Codes	
Dist	Mail Order
Special	
A-1	

Blank

## CONTENTS

	Page
1. INTRODUCTION .....	7
2. THEORY .....	7
2.1 Material and Energy Balances .....	7
2.2 Stage Model Approach .....	10
2.3 Equilibrium Theory .....	11
3. MATERIALS AND METHODS .....	13
4. RESULTS AND DISCUSSION .....	14
4.1 Water on Activated Carbon .....	14
4.2 Breakthrough of 50% RH Feed To A Clean Bed .....	16
4.3 Breakthrough of 80% RH Feed To Bed Equilibrated At 50% RH .....	18
4.4 Breakthrough of 80% RH Feed To A Clean Bed .....	18
5. CONCLUSIONS .....	19
NOTATION .....	21
LITERATURE CITED .....	29

## LIST OF FIGURES

	Page
1. Schematic of Breakthrough Apparatus .....	22
2. Path In Modified Isotherm Plane 50%RH, 80%RH Feed To Clean Bed And 80%RH Feed to 50%RH Bed of BPL .....	23
3. Enlargement of Path In Modified Isotherm Plane 50%RH, 80%RH Feed To Clean Bed Of BPL .....	24
4. Breakthrough of Water Vapor On BPL Carbon 50%RH Feed To Clean Bed .....	25
5. Breakthrough Of Water Vapor On BPL Carbon 80%RH Feed To Bed Equilibrated To 50%RH .....	26
6. Breakthrough Of Water Vapor On BPL Carbon 80%RH Feed To Clean Bed .....	27

## LIST OF TABLES

	Page
1. Breakthrough Experiment Conditions .....	15
2. Heat Capacities .....	15

# THE DYNAMIC BEHAVIOR OF WATER VAPOR ON ACTIVATED CARBON

## 1. INTRODUCTION

Water adsorption on activated carbon is of particular interest for air purification applications where contaminants must be removed from humid air. Water vapor adsorption can limit filter performance against challenges of light gases by displacing previously adsorbed contaminants or by reducing the available adsorption space. A complete understanding of the single component adsorption behavior of water vapor on activated carbon can serve as a basis to develop a theory for multicomponent behavior. This study considers in detail the adsorption of water on BPL activated carbon.

The adsorption behavior of any vapor on an adsorbent can be understood through the adsorption equilibrium relationship and the material and energy balances. Water adsorption on activated carbon exhibits a pronounced hysteresis that complicates the analysis of desorption. Doong and Yang<sup>1</sup> present a model for multicomponent adsorption of water and hydrocarbons on activated carbon including equilibrium and adsorber dynamics. Their work, however, neglects the energy balance and does not present data on breakthrough runs. The purpose of this paper is to develop and solve the material and energy balance equations so the results can be compared to actual breakthrough experiments. The results presented here for adsorption dynamics can be extended to desorption dynamics. Two approaches to analyzing the water adsorption process on activated carbons are considered. These are the stage model approach and the equilibrium theory approach. In both cases a mathematical model is used to describe the dynamic behavior of water vapor challenging a bed of activated carbon. Three breakthrough experiments are performed that result in three different types of waves. The characteristics of each wave type and their impact on filter performance are discussed.

## 2. THEORY

### 2.1 Material and Energy Balances.

The equations to describe water adsorption on activated carbon should include material and energy balances as well as the equilibrium relationship. The easiest way to develop these equations is to describe the bed as consisting of a solid phase and a vapor phase. The stationary(solid) phase consists of the solid porous

particles and the adsorbate. The vapor phase consists of the inert carrier gas and the adsorbable vapor in both the interstices of the bed and the pores of the particles.

The governing differential equations for the conservation of mass and energy respectively, neglecting dispersion and channeling, of a fixed-bed adsorber can be written as follows:

$$\epsilon \frac{\partial vc}{\partial z} + \epsilon \frac{\partial c}{\partial t} + \rho_b \frac{\partial q}{\partial t} = 0 \quad (1)$$

$$\epsilon \frac{\partial(v\rho_f h_f)}{\partial z} + \epsilon \frac{\partial(\rho_f h_f)}{\partial t} + \rho_b \frac{\partial h_s}{\partial t} = -U \Delta T \quad (2)$$

The fluid phase and stationary phase enthalpies are defined by:

$$h_f = c_f(T - T_{ref}) \quad (3)$$

$$h_s = (c_s + c_a q)(T - T_{ref}) - \int_0^q \lambda dq \quad (4)$$

Here  $c$  is the vapor concentration,  $q$ , the adsorbed phase concentration in moles of adsorbate per unit mass of adsorbent,  $T$ , the temperature,  $z$ , the distance down the tube length,  $t$ , the time,  $\epsilon$ , the void fraction of the bed, and  $U$ , the overall heat transfer coefficient of the filter tube.

The rate at which material is transferred from the passing vapor stream to the surface of the carbon is governed by a film mass transfer resistance which can be written as follows:

$$\rho_b \frac{\partial q}{\partial t} = (k_v a) (c - c^*) \quad (5)$$

Equation 5 assumes Glueckauf's linear driving force, where  $c^*$  is the vapor phase concentration at the surface of the particle.

Dimensionless variables can be introduced to simplify equations 1, 2, 5:

$$\tau = \frac{\epsilon v_o t}{L} \quad \zeta = \frac{z}{L} \quad v^* = \frac{v}{v_o} \quad (6,7,8)$$

$$U' = \frac{2 U L}{\epsilon v_o r_i} \quad (9)$$

$$(k_v a)' = k_v a \frac{L}{\epsilon v_o} \quad (10)$$

The choice of the dimensionless parameter  $\tau$  has special physical significance. It represents the number of superficial column volumes that have been fed to the bed at any given time.

In evaluating solutions, parameters appearing in equations 1, 2, and 5 can be treated as functions of concentration and temperature. However, to simplify the development, several assumptions can be made, namely:

- (a) all heat capacities are constant with mean values taken.
- (b) the vapor phase is ideal and the effect of composition on the vapor-phase density and velocity is small.
- (c) the adsorption process considered here occurs at low gas phase concentrations so that the effect on velocity and density is negligible.

Thus, the dimensionless velocity and the fluid density can be written as:

$$v^* = \frac{T}{T_o} \quad \rho_f = \rho_{fo} \frac{T_o}{T} \quad (11,12)$$

For adsorption processes involving gases at low to moderate pressures (which would be typical of all air purification applications) the rate of accumulation in the vapor phase is small compared to the accumulation in the solid phase. This leads to the elimination of the second term in equations 1 and 2. The system of governing differential equations may then be expressed as:

$$\frac{\partial(v^* c)}{\partial \zeta} + \rho_b \frac{\partial q}{\partial \tau} = 0 \quad (13)$$

$$\frac{\partial(v^* \rho_f h_f)}{\partial \zeta} + \rho_b \frac{\partial h_s}{\partial \tau} = -U' \Delta T \quad (14)$$

$$\rho_b \frac{\partial q}{\partial \tau} = (k_v a)' (c - c^*) \quad (15)$$

Equations 13, 14, and 15 are three independent equations with four dependent variables ( $c$ ,  $c^*$ ,  $q$ ,  $T$ ). Another equation is required in order to specify the system, namely the adsorption equilibrium relationship:

$$q = f(c^*, T) \quad (16)$$

The solution to equations 13 - 15 with 16 requires the imposition of appropriate initial and boundary conditions. For systems considered here the initial bed state and the feed concentration are constant throughout the experiment. Mathematically this can be expressed as:

$$\begin{aligned} c &= c_0 \quad \text{and} \quad T = T_0 \quad \text{at } \tau = 0 \quad \text{for } 0 < \zeta < 1 \\ c &= c_{\text{feed}} \quad \text{and} \quad T = T_{\text{feed}} \quad \text{at } \zeta = 0 \quad \text{for all } \tau > 0 \end{aligned} \quad (17)$$

Two approaches are taken to solve the governing set of differential equations, 13 - 15, with 16: the stage model and equilibrium theory. The stage model is more flexible and can easily treat systems with non-constant initial and boundary conditions. Generally, equilibrium theory is more insightful about the nature of the adsorption waves, however, it cannot be used where mass and heat transfer effects must be considered. Both techniques are presented here in order to gain a complete understanding of the process.

## 2.2 Stage Model Approach.

Equations 13 - 15 when coupled with the equilibrium relationship 16 can be reduced to a set of ordinary differential equations using a stage model approach.<sup>2,3</sup> Each stage is considered to be well mixed with the effluent concentration and temperature of stage  $i$  used as the feed concentration of stage  $i+1$ . Friday and LeVan<sup>4</sup> have reported a successful method for reducing the partial differential equations 13 - 15 to ordinary differential equations by writing the spatial derivatives in equations 13 and 14 in finite difference form using backward differences.

$$\frac{dq_i}{d\tau} = \frac{1}{\rho_b \Delta \varsigma} \left[ (v^* c)_{i-1} - (v^* c)_i \right] \quad (18)$$

$$\begin{aligned} \frac{dT_i}{d\tau} = & \frac{1}{\rho_b (c_s + c_a q_i)} \left\{ \frac{\rho_{fo} c_f}{\Delta \varsigma} (T_{i-1} - T_i) \right. \\ & \left. - \rho_b [c_a (T_i - T_{ref}) - \lambda_i] \frac{dq_i}{d\tau} - U' \Delta T \right\} \end{aligned} \quad (19)$$

The resulting equations 18 and 19 are solved using a Runge-Kutta 4th order integration algorithm with twenty stages.

### 2.3 Equilibrium Theory.

The development of the equilibrium theory solution requires the mass and heat transfer resistances to be negligible. Therefore, the driving force terms on the right side of equations 14 and 15 are set to zero.

The equilibrium theory solution to 13, 14 and 16 requires the use of the method of characteristics that has been presented by numerous authors.<sup>5-10</sup> If concentration of the material in the bed can be expressed as a function of distance and time by,

$$c = f(\varsigma, \tau) \quad (20)$$

then the total differential of c can be written as:

$$dc = \frac{\partial c}{\partial \varsigma} d\varsigma + \frac{\partial c}{\partial \tau} d\tau \quad (21)$$

The solution along regions of constant concentration require that  $dc=0$  so that equation 19 can be rearranged.

$$\frac{d\varsigma}{d\tau} = - \frac{\partial c / \partial \tau}{\partial c / \partial \varsigma} \quad (22)$$

Now the material balance equation 13 can be rewritten when the equilibrium relationship 16 is substituted for the partial of q with respect to time.

$$\frac{\partial c}{\partial \zeta} + \rho_b \frac{dq}{d(v^* c)} \frac{\partial c}{\partial \tau} = 0 \quad (23)$$

Equation 23 can be rearranged into a form compatible with the right hand side of equation 22.

$$-\frac{dc/d\tau}{dc/d\zeta} = \frac{1}{\rho_b} \frac{d(v^* c)}{dq} \quad (24)$$

When equation 24 is substituted into equation 22 the following expression for the characteristic direction is obtained.

$$\frac{d\zeta}{d\tau} = \frac{1}{\rho_b} \frac{d(v^* c)}{dq} \quad (25)$$

The left hand side of equation 25 represents the speed with which a given concentration travels down the bed, while the right hand side of equation 25 is the slope of the equilibrium relationship.

The energy balance when written without the heat transfer resistance takes the following form:

$$\frac{\partial(v^* \rho_f h_f)}{\partial \zeta} + \rho_b \frac{\partial h_s}{\partial \tau} = 0 \quad (26)$$

Using the same procedure as for the material balance, the characteristic equation takes the following form:

$$\frac{d\zeta}{d\tau} = \frac{1}{\rho_b} \frac{d(v^* \rho_f h_f)}{dh_s} \quad (27)$$

The material and energy balances can be combined for the initial value problem to provide:

$$\frac{\tau}{\varsigma} = \rho_b \frac{dq}{d(v^* c)} = \rho_b \frac{dh_s}{d(v^* \rho_f h_f)} \quad (28)$$

The two enthalpy terms on the right of equation 28 can be written as functions of  $q$  and  $T$ . Thus equation 28 can be rearranged in terms of the directional derivative  $dq/dT$  to take the following form:

$$\left[ \frac{\partial(v^* c)}{\partial q} \frac{\partial h_s}{\partial q} \right] \left( \frac{dq}{dT} \right)^2 + \left[ \frac{\partial(v^* c)}{\partial q} \frac{\partial h_s}{\partial T} + \frac{\partial(v^* c)}{\partial T} \frac{\partial h_s}{\partial q} \right. \\ \left. - \frac{d(v^* \rho_f h_f)}{dT} \right] \frac{dq}{dT} + \frac{\partial(v^* c)}{\partial T} \frac{\partial h_s}{\partial T} = 0 \quad (29)$$

Equation 29 is a quadratic in  $dq/dT$ . The two solutions correspond to the characteristics emanating from a given point of  $c$ ,  $q$ , and  $T$ . By starting from the initial and feed conditions the solution to equation 29 is obtained. The resulting slopes are then plotted in the hodograph planes of  $q$  versus  $T$  and the  $q$  versus  $v^* c$  until the characteristics intersect. Implementation of equilibrium theory to obtain the breakthrough curves requires adherence to two rules. A wave must be gradual if possible. Slopes in the  $v^* c$  plane must increase from initial bed condition to feed condition. If the slope of the characteristic does not increase continuously in going from initial to feed conditions then the larger concentrations would overrun the smaller concentrations. This is an impossible situation. Earlier studies by Devault<sup>11</sup> and Lax<sup>12</sup> showed that these conditions result in the formation of a shock. The shock path must satisfy the material and energy balances as given by the following relationship:

$$\frac{\tau}{\varsigma} = \rho_b \frac{\Delta q}{\Delta(v^* c)} = \rho_b \frac{\Delta h_s}{\Delta(v^* \rho_f h_f)} \quad (30)$$

This is similar to equation 28 except that here a chord, rather than the slope of the characteristic, is used to determine the speed of the wave in the bed.

### 3. MATERIALS AND METHODS

The apparatus used for the breakthrough experiments is shown in Figure 1. Air, used as the carrier gas, passes through a molecular sieve dryer and a carbon filter to remove water and organics. The main metering valve regulates the flow. After the clean air passes through the flowmeter, a portion of the stream is

saturated in a water bath. The desired relative humidity is achieved in the following manner. The metering valve and the bypass valve are set such that the ratio of the their flows produces a relative humidity near the desired value. The humidity analyzer and controller (EG&G 911 Digital Humidity Analyzer) measures the relative humidity of the feed stream based on the temperature of the feed stream. If the relative humidity is below the setpoint, the water bath heater is activated. Since, it is a simple on-off controller with no cooling action, the initial setting of the bypass flow must produce a lower than desired RH. The humidified air flows through the carbon bed and the effluent relative humidity is measured by a second EG&G humidity analyzer. Periodically during each breakthrough run the bed was removed from the flowing air stream in order to weigh it.

The carbon sample used was 12x30 mesh BPL Lot #7502. Calgon literature states that the bulk density of the carbon is  $480 \text{ kg/m}^3$ . The particle diameter is taken to be 0.001 m. The sample for each experiment is dried for at least two days at  $110^\circ\text{C}$ . The carbon is then poured into a 0.0415 m diameter plexiglass tube to give a bed depth of approximately 4 cm. The overall heat transfer coefficient of the plexiglass is taken to be  $0.093 \text{ kJ/m}^2 \text{ K s}$ .

#### 4. RESULTS AND DISCUSSION

##### 4.1 Water On Activated Carbon.

The breakthrough concentration and temperature have been measured using the following feed and initial bed conditions: 50% RH feed to a clean bed, 80% RH feed to a bed equilibrated at 50% RH, 80% RH feed to a clean bed. These conditions have been chosen to illustrate the three different wave types that can be formed in an adsorption bed. Rhee et al.<sup>6</sup> describe the three wave types as gradual, abrupt and combined in their equilibrium theory analysis. The important features of each are discussed as each experiment is analyzed. Table 1 is a summary of the operating conditions for each experiment. Table 2 lists the heat capacity values used in this study.

TABLE 1. Breakthrough Experiment Conditions

Experiment	Feed		Initial Bed Conditions			v (m/sec)	T <sub>amb</sub> (K)
	RH%	T(K)	RH%	T(K)	Carbon(g)		
1	50	298	0	297.5	23.96	.0616	297.5
2	80	297	50	297	23.96	.0616	297
3	80	298	0	298	25.85	.123	298

TABLE 2. Heat Capacities

$$c_a = 1.04 \text{ kJ/kg K}$$

$$c_s = 2.7 \text{ kJ/kg K}$$

$$c_f = 0.075 \text{ kJ/kg K}$$

$$T_{ref} = 298^{\circ} \text{ K}$$

In order to implement the stage model and the equilibrium theory model the form of the equilibrium relationship must be established. It is proposed that a modification to the Hacskaylo-LeVan isotherm<sup>13</sup> would give a reasonable fit to the data. The form of the equation is as follows:

$$\ln(p) = A' - \frac{B'}{C' + T} \quad (31)$$

where

$$A' = A + (K1\theta + 1)\ln(\theta) \quad B' = B \quad C' = C + K2(1 - \theta) \quad (32)$$

and

$$\theta = \frac{q}{q_{sat}} \quad (33)$$

$$\lambda = RT^2 \left( \frac{\partial \ln(p)}{\partial T} \right)_q = RT^2 \frac{B'}{(C' + T)^2} \quad (34)$$

The following values are used for water adsorption on BPL:

$$A = 18.3036 \quad B = 3816.44 \quad C = -46.13$$

$$K1 = 2.56 \quad K2 = 37.9 \quad q_{sat} = 0.0217$$

The Antoine parameters, taken from Reid et al.,<sup>14</sup> give the vapor pressure in millimeters of mercury. The isotherms of water on BPL have been measured previously by Mahle and Friday<sup>15</sup> over the temperature range 15 - 35 °C. Only adsorption data is considered here; desorption is not considered. The result of correlating the adsorption data using equations 31 - 33 is presented in Figures 2 and 3 in the modified isotherm plane of  $q$  versus  $v^* c$ . Figure 3 is an enlargement of Figure 2 in the low loading region.

The value of  $k_v$ , the mass transfer coefficient, can be calculated using the Sherwood number correlation of Ranz and Marshall.<sup>16</sup> Calgon literature indicates that an appropriate value for  $a$ , the surface to volume ratio, is 3400 m<sup>-1</sup>.

#### 4.2 Breakthrough of 50% RH Feed To A Clean Bed.

The breakthrough results for a challenge of 50% RH(0.628 mol/m<sup>3</sup> at 298 °K) air to clean bed correspond to a region of the isotherm that is unfavorable for adsorption. The effluent concentration and temperature are plotted as a function of time in Figure 4. The effluent concentration versus time curve is typical of a gradual wave. The breakthrough curve is concave downward to the time axis. After a short period of time, an appreciable percentage of the feed concentration is seen in the effluent. The temperature response is also typical of a gradual wave. The temperature quickly rises to a maximum (in this case about 305 °K) and then falls gradually back to the feed temperature.

Construction of solutions using equilibrium theory requires the use of the two rules stated earlier. A wave will be gradual if possible. Slopes in the  $q$  versus  $v^* c$  plane must increase from initial to feed conditions. There are two sets of characteristics corresponding to two roots of the equation 29. The two

characteristic curves are required in order to obtain the path that connect any initial condition to any feed condition. The 1 wave is the first wave to leave the bed, therefore it must be the wave connected to the initial condition while the 2 wave is connected to the feed.

The slope of the 1 characteristic on the  $q$  versus  $v^*$  plane is decreasing from the initial condition, a clean bed. This means there will be a shock path that leaves this point. This is shown as the bottom dotted line in Figure 2 and the upper dotted line in Figure 3 emanating from the origin. The 2 wave that connects the feed condition, 50% RH, has a constantly increasing slope from initial to feed condition corresponding to a gradual wave represented by the bold solid line in Figures 2 and 3. The point where the shock from the initial condition and gradual wave meet can be found by stepping out in temperature along each path using equations 29 and 30 until they intersect. This corresponds to a plateau concentration. Figures 2 and 3 make it easy to visualize how the solution path cuts across isotherms producing a temperature wave.

There is very close agreement between the stage model, the equilibrium theory model, and the data as seen in Figure 4. The equilibrium theory solution does predict a larger temperature rise than the stage model. This is expected because equilibrium theory assumes adiabatic behavior. The actual recorded temperature does not reach as high as the prediction because during the first minutes of the run the sample tube was periodically taken off line so that the water uptake could be recorded. Note that both the concentration and the temperature wave travel with the same velocity as seen in Figure 4. This is predicted by equilibrium theory using equation 28.

A preliminary study, using only isothermal equilibrium theory, did not fit the data indicating that the effect of temperature is very important to this process. There is a gradual wave associated with the low RH for the isothermal case. However, the shock associated with temperature tends to overrun these gradual wave characteristics in the adiabatic case leading to a shock in temperature and concentration. Note that because the water isotherm is unfavorable at lower RH these low concentrations tend to run out of the column quickly. The large temperature rise associated with the 1 wave has the effect of removing water from the bed that was just adsorbed at the lower temperature. This increases the required time for complete saturation of the bed. It appears that isothermal adsorption would provide a faster means of achieving saturation.

#### 4.3 Breakthrough of 80% RH Feed To Bed Equilibrated At 50% RH.

The water isotherm is favorable between 50% RH( $0.628 \text{ mol/m}^3$  at  $298^\circ\text{K}$ ) and 80% RH( $1.001 \text{ mol/m}^3$  at  $298^\circ\text{K}$ ) as seen in Figure 2. This is the typical shape of an adsorption isotherm, and one could expect the standard S-shaped breakthrough curve. Figure 5 shows the results of an 80% RH feed to a bed initially equilibrated at 50% RH. Although the shape of this curve is not very sharp, the breakthrough behavior does follow an S-shaped pattern.

This S-shaped pattern is called an abrupt wave or a constant pattern wave. This means that at a certain distance into the bed, the shape of the concentration front does not change as the wave is transmitted down the bed. There is also an initial shock characterized primarily by a temperature rise.

Referring back to Figure 2, the 2 characteristic emanating from the feed of 80% RH and the 1 characteristic from the initial concentration of 50% RH both violate the gradual wave criterion. The slopes of these waves decrease from initial to feed conditions, therefore each of these waves must start as a shock. The equilibrium theory solution then requires that equation 30 be solved from both the initial and feed conditions until they intersect, while at each increment checking to see whether the slope of the gradual wave is continuing to violate the gradual wave criterion. The intersection point leads to a plateau condition. This path is close to having a gradual portion because it is so close to the inflection point of the isotherm. However, the adiabatic nature of this system results in the formation of two shocks.

The simulation provided by the stage model and equilibrium theory represent the data well for this run. The resulting breakthrough behavior is shown in Figure 5. Equilibrium theory provides a very accurate measure of the center of both the concentration and temperature waves. The plateau region between the two shock fronts is apparent in the data. Again the temperature rise measured in the experiment is reduced due to sampling of the uptake weight of the bed. The effect of the mass and heat transfer resistances in the stagemodel becomes obvious in the shock portion of the breakthrough curves. These resistances tend to spread out the shock wave in an actual experiment.

#### 4.4 Breakthrough of 80% RH Feed To A Clean Bed.

The water isotherm changes from unfavorable to favorable between 50% RH and 80% RH. The effect of this inflection in the isotherm should be apparent on the breakthrough behavior. Figure 6 shows the breakthrough data measured for 80% RH feed to a clean bed. Notice that the resulting breakthrough curves of both

temperature and concentration are essentially a combination of the first two experiments. The only difference is the faster flow rate (10 l/min as opposed to 5 l/min).

The equilibrium theory solution path is characterized by an initial 1 wave shock as in the run with 50% RH feed to a clean bed, the lower dotted line in Figure 3. There is also a shock emanating from the feed as in the run with 80% RH feed to a bed equilibrated to 50% RH. However there is a third transition. As the isotherm changes from favorable to unfavorable a combined wave is formed that shows both shock and gradual wave behavior, Figure 2. It is possible to identify this as a combined transition because it does not have a plateau region where the two waves unite. There is a portion of the gradual wave for 80% RH feed to clean bed that parallels the shock path for 80% RH feed to a bed equilibrated at 50%RH. The two runs are not identical over the same range of RH. This result only becomes apparent in the adiabatic analysis.

The shape of both the concentration and temperature profiles agrees with the stage model and equilibrium theory predictions. The subtle shape of the combined transition is not obvious from the data. Equilibrium theory allows this combined transition to be identified.

## 5. CONCLUSIONS

- The three types of waves that can be formed in and passed through an adsorption bed are demonstrated both mathematically and experimentally.
- The stage model seems to fairly represent the breakthrough using correlated equilibrium data and *a priori* calculated rate parameters.
- Equilibrium theory allows the exact nature of the transitions to be explored.
- The inability of equilibrium theory to be used with heat and mass transfer resistances leads to some discrepancy between this method and the experimental results.

Blank

## NOTATION

---

$a$	= surface to volume ratio( $m^{-1}$ )
$A, B, C$	= Antoine equation parameters( $p_{sat}$ in mm Hg)
$c_*$	= gas phase concentration of water( $mol/m^3$ )
$c$	= gas phase concentration of water in the pellet( $mol/m^3$ )
$c_a$	= heat capacity of adsorbed phase( $kJ/kgK$ )
$c_f$	= heat capacity of gas phase( $kJ/kgK$ )
$c_s$	= heat capacity of solid phase( $kJ/kgK$ )
$h_f$	= enthalpy of gas phase( $kJ/kg$ )
$h_s$	= enthalpy of solid phase( $kJ/kg$ )
$k_v$	= mass transfer coefficient( $m/s$ Ref. 16)
$K_1, K_2$	= coefficients of water adsorption isotherm, Eq. (32)
$L$	= length of bed( $m$ )
$p$	= partial pressure of water(Torr)
$q$	= solid phase concentration( $mol/kg$ )
$q_{sat}$	= solid phase concentration at saturation( $mol/kg$ )
$r_i$	= inner radius of filter tube( $m$ )
$R$	= gas constant
$t$	= time
$T$	= temperature( $K$ )
$T_o$	= temperature of feed gas( $K$ )
$T_{ref}$	= heat capacity reference temperature( $K$ )
$U$	= overall heat transfer coefficient of filter tube( $kJ/m^2Ks$ )
$v$	= interstitial velocity( $m/s$ )
$v_o$	= interstitial velocity of feed( $m/s$ )
$z$	= axial distance coordinate( $m$ )
$\epsilon$	= void fraction of packing
$\zeta$	= dimensionless axial coordinate, Eq. (7)
$\theta$	= fractional saturation of the bed
$\lambda$	= heat of adsorption( $kJ/mol$ )
$\rho_b$	= bulk density of packing( $kg/m^3$ )
$\rho_f$	= density of gas phase( $kg/m^3$ )
$\rho_{fo}$	= density of inlet gas ( $kg/m^3$ )
$\tau$	= dimensionless time, Eq. (6)

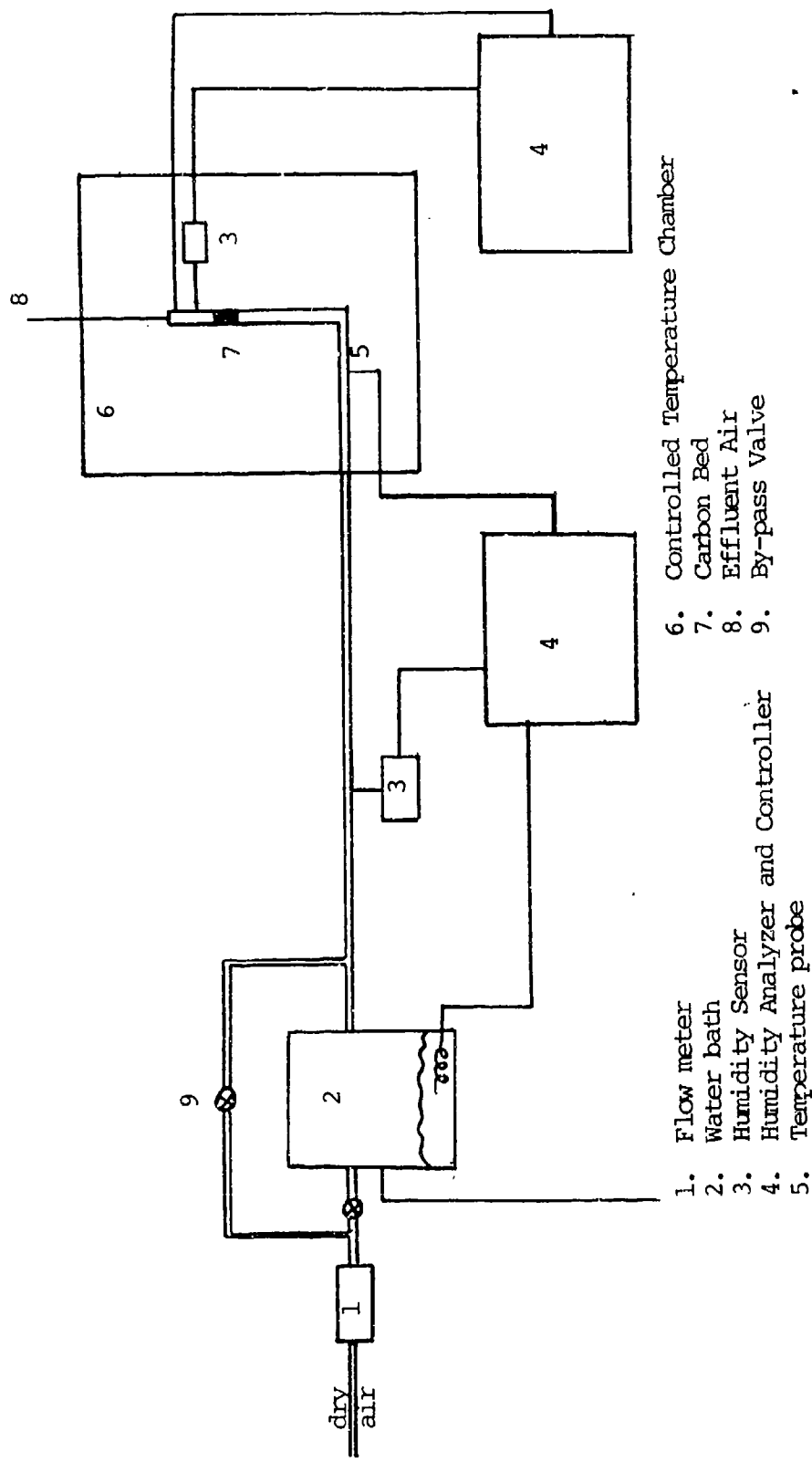
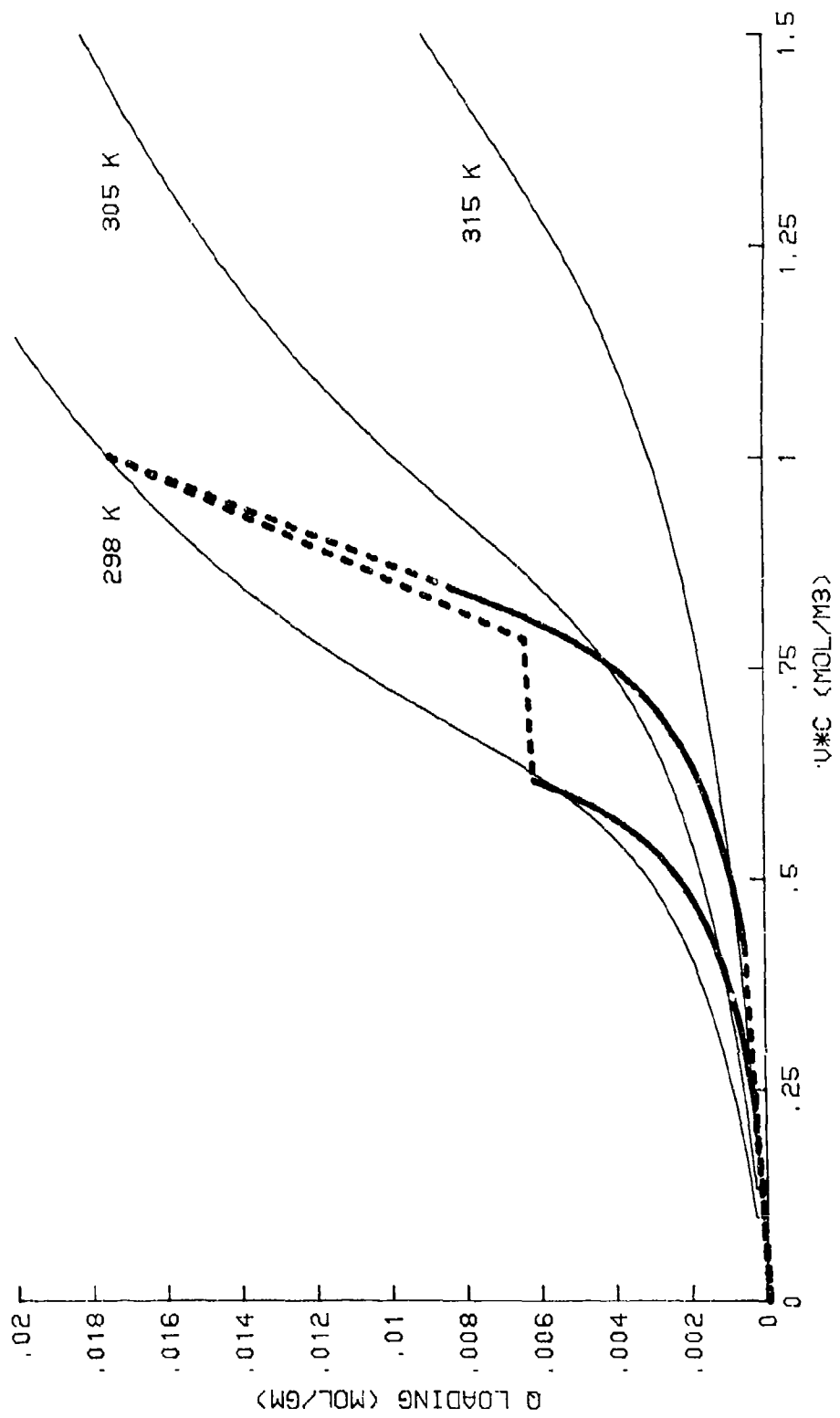


Figure 1. Schematic of Breakthrough Apparatus



Path In Modified Isotherm Plane  
 50%RH, 80%RH Feed To Clean Bed  
 And 80%RH Feed To 50%RH Bed Of BPL

Figure 2.

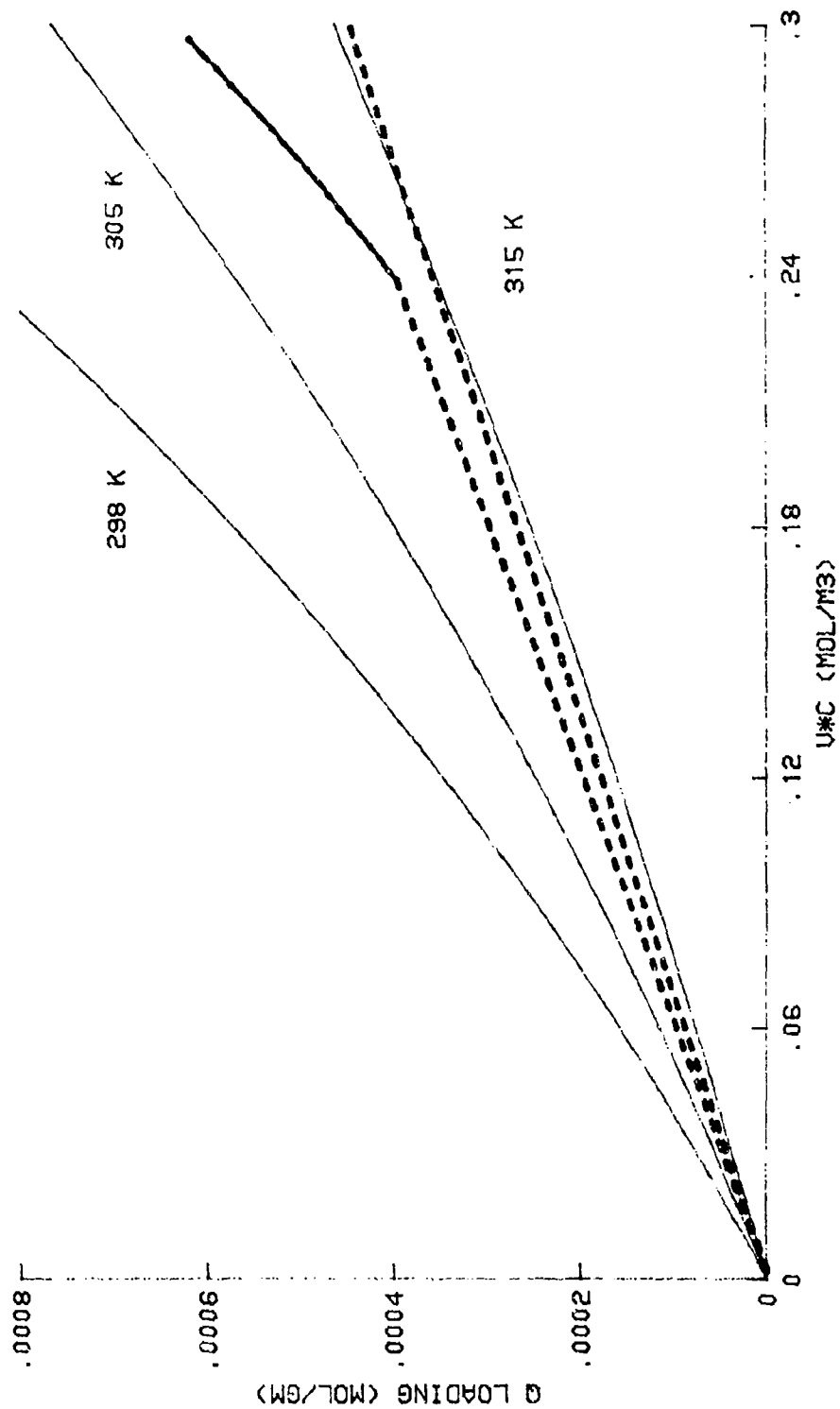


Figure 3. Enlargement Of Path In Modified Isotherm Plane  
50%RH, 80%RH Feed To Clean Bed Of BPL

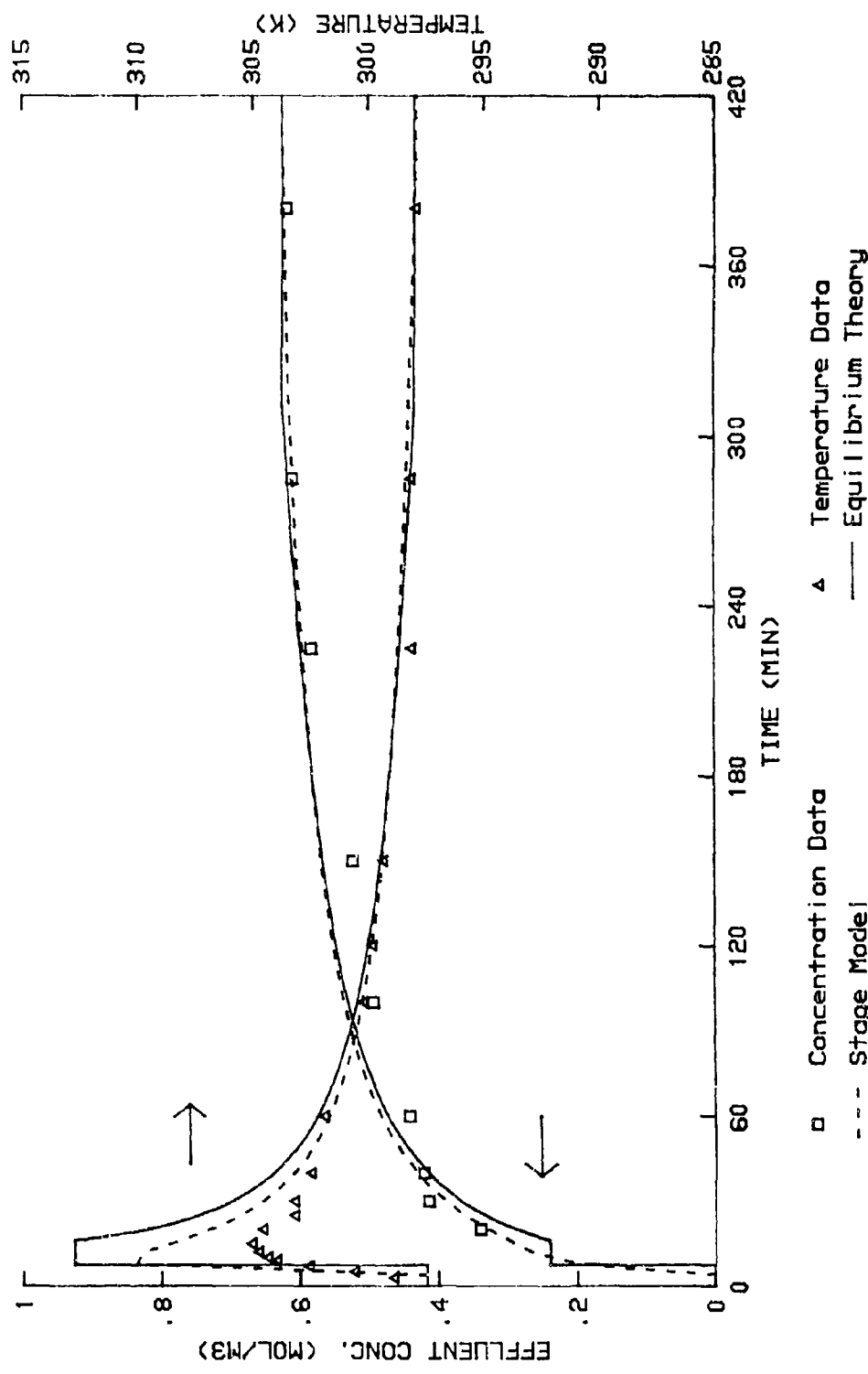


Figure 4. Breakthrough Of Water Vapor On BPL Carbon 50%RH Feed To Clean Bed

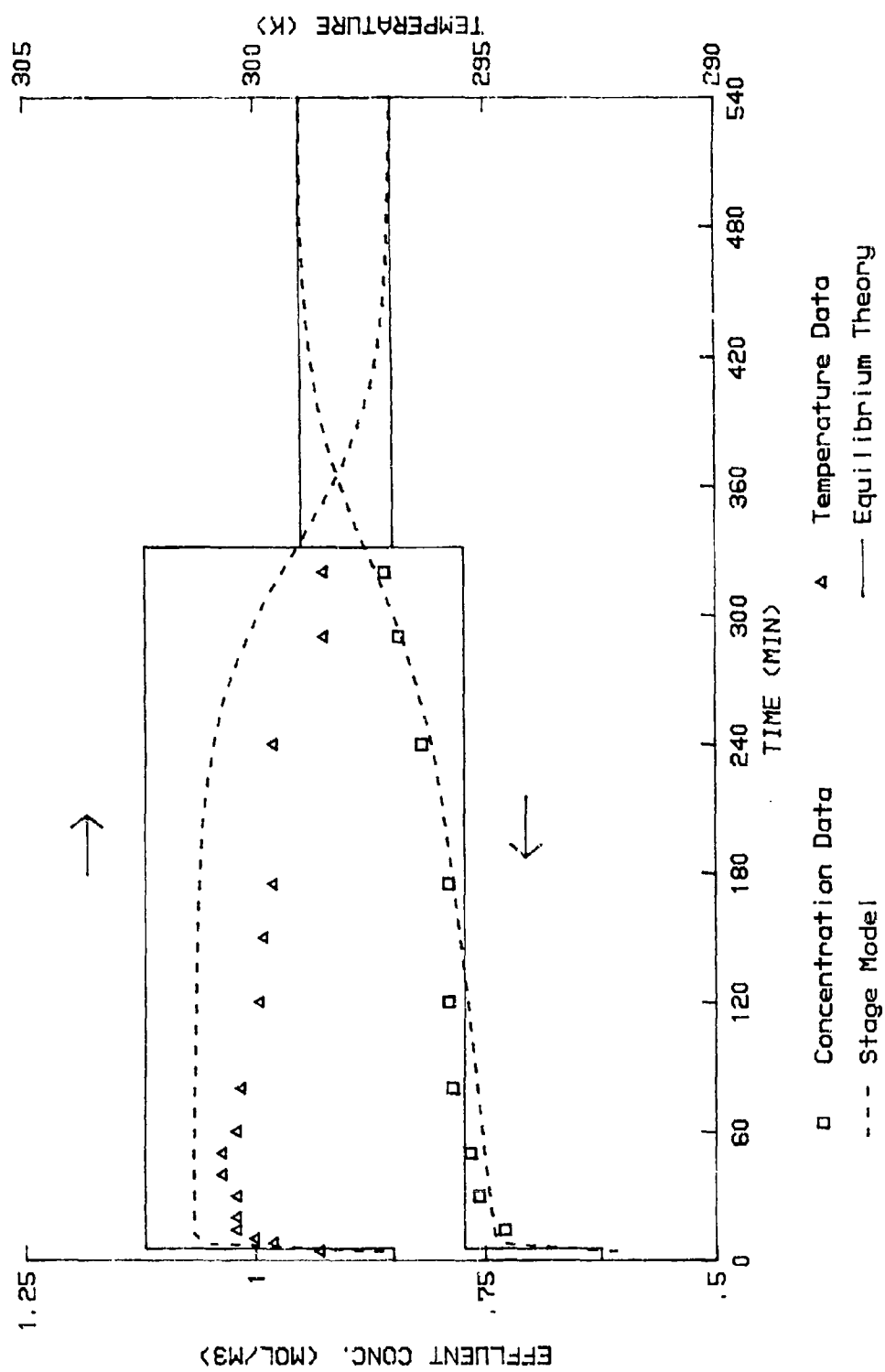


Figure 5.

Breakthrough Of Water Vapor On BPL Carbon  
80%RH Feed To Bed Equilibrated To 50%RH

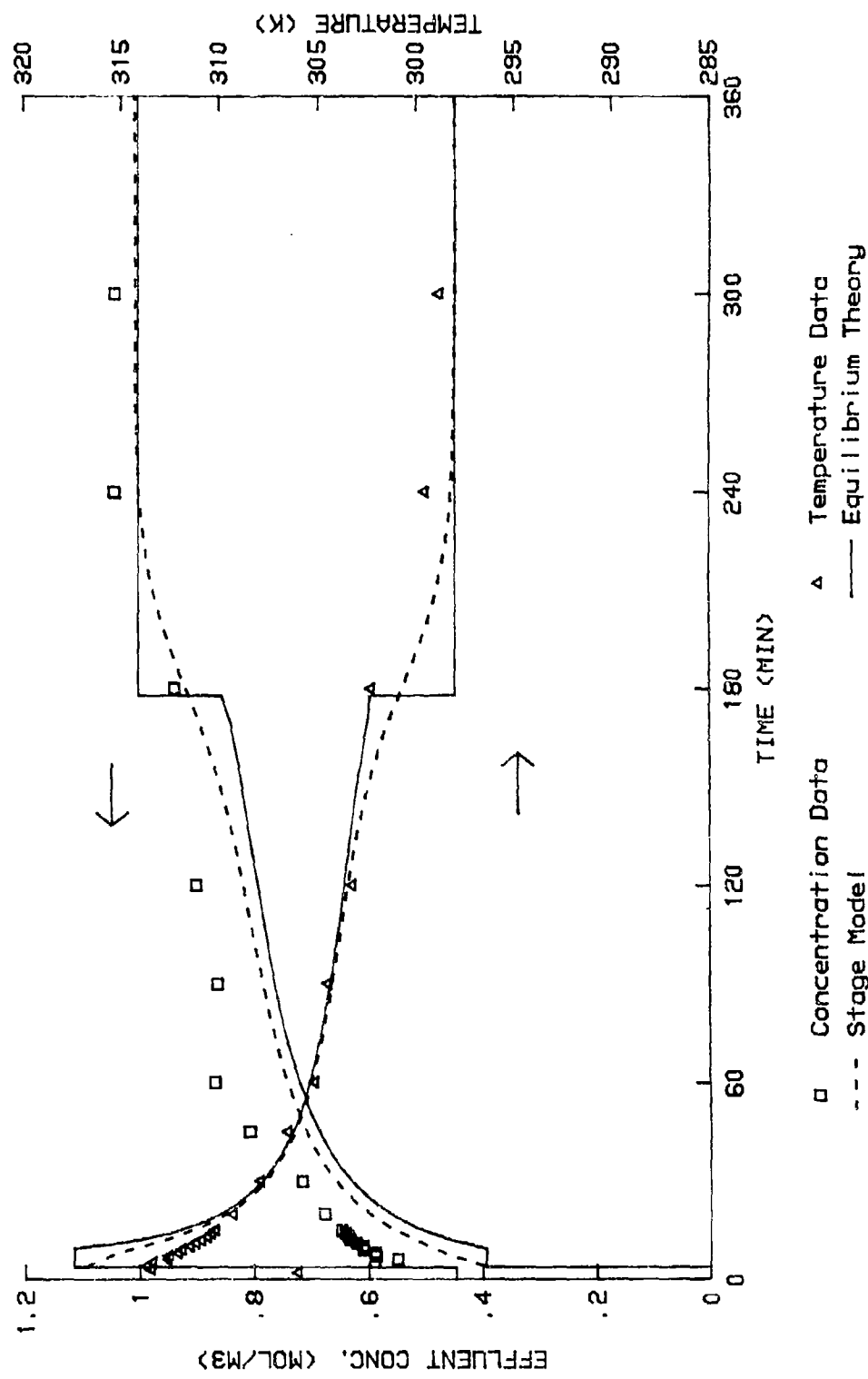


Figure 6.  
Breakthrough Of Water Vapor On BPL Carbon  
80%RH Feed To Clean Bed

Blank

## LITERATURE CITED

1. Doong, S.J., and Yang, R.T., "Adsorption of Mixtures of Water Vapor and Hydrocarbons By Activated Carbon Beds: Thermodynamic Model for Adsorption Equilibrium and Adsorber Dynamics," *AICHE Symposium Series: Adsorption and Ion Exchange* vol. 259(83), p. 87 (1987).
2. Rodrigues, A.E. and Beira, E.C., "Staged Approach of Percolation Processes," *AICHE J.* vol. 25, p. 416 (1976).
3. Ikeda, K., "Performance of the Nonisothermal Fixed-Bed Adsorption Column with Nonlinear Isotherms," *Chem. Eng. Sci.* vol. 34, p. 941 (1981).
4. Friday, D.K., and LeVan, D., "Solute Condensation in Adsorption Beds During Thermal Regeneration," *AICHE J.* vol. 28, p. 86 (1982).
5. Friday, D.K., and LeVan, D., "Thermal Regeneration of Adsorption Beds: Equilibrium Theory for Solute Condensation," *AICHE J.* vol. 30, p. 679 (1984).
6. Acrivos, A., "Method of Characteristics Technique: Application to Heat and Mass Transfer Problems," *Ind. Eng. Chem.* vol. 48, p. 703 (1956).
7. Pan, C. Y., and Basmadjian, D., "Constant Pattern Adiabatic Fixed-Bed Adsorption," *Chem. Eng. Sci.* vol. 22, p. 285 (1967).
8. Pan, C.Y., and Basmadjian, D., "An Analysis of Adiabatic Sorption of Single Solutes in Fixed Beds: Equilibrium Theory," *Chem. Eng. Sci.* vol. 26, p. 45 (1971).
9. Rhee, H.K., Aris, R. and Amundson, N.R., *First Order Partial Differential Equations: Volume I, Theory and Applications of Single Equations*, pp. 188-410, Prentice-Hall, Englewood Cliffs, NJ, 1986.
10. Ruthven, D.M., *Principles of Adsorption and Adsorption Processes*, pp. 274-323, John Wiley and Sons, New York, NY 1984.
11. DeVault, D., "The Theory of Chromatography," *J. Amer. Chem. Soc.* vol. 65, p. 532 (1943).
12. Lax, P.D., "The Formation and Decay of Shock Waves," *Amer. Math. Monthly* vol. 79, p. 227 (1972).

13. Hacskaylo, J.J., and LeVan, M.D., "Correlation of Adsorption Equilibrium Data Using a Modified Antoine Equation: A New Approach for Pore-Filling Models," *Langmuir* vol. 1, p. 97 (1987).
14. Reid, R.C., Prausnitz, J.M., and Sherwood, T.K., *The Properties of Gases And Liquids*, 3rd ed., p. 634, McGraw-Hill, New York, NY, 1977.
15. Mahle, J.J., and Friday, D.K., *Water Adsorption Equilibria On Microporous Carbons*, CRDEC-TR-018, U.S. Army Chemical Research, Development and Engineering Center, Aberdeen Proving Ground, MD, November 1988, UNCLASSIFIED REPORT.
16. Ranz, W.E. and Marshall, W.R., "Evaporation From Drops Part II," *Chem. Eng. Prog.* vol. 48, p. 173 (1952).